Amino Acids (2013) 45:989–1002
DOI 10.1007/s00726-013-1556-3

ORIGINAL ARTICLE

Transport of asymmetric dimethylarginine (ADMA) by cationic amino acid transporter 2 (CAT2), organic cation transporter 2 (OCT2) and multidrug and toxin extrusion protein 1 (MATE1)

Joachim Strobel · Fabian Müller · Oliver Zolk · Beate Endreß · Jörg König · Martin F. Fromm · Renke Maas

Received: 8 April 2013 / Accepted: 1 July 2013 / Published online: 18 July 2013

Abstract Asymmetric dimethylarginine (ADMA), inhibiting the nitric oxide (NO) synthesis from L-arginine, is a known cardiovascular risk factor. Our aim was to investigate if ADMA and/or L-arginine are substrates of the human cationic amino acid transporters 2A (CAT2A, *SLC7A2A*) and 2B (CAT2B, *SLC7A2B*), the organic cation transporter 2 (OCT2, *SLC22A2*), and the multidrug and toxin extrusion protein 1 (MATE1, *SLC47A1*). We systematically investigated the kinetics of ADMA and L-arginine transport in human embryonic kidney (HEK293) cells stably overexpressing CAT2A, CAT2B, OCT2, or MATE1. Vector-only transfected HEK293 cells served as controls. Compared to vector control cells, uptake of ADMA and L-arginine was significantly higher ($p < 0.05$) in cells expressing CAT2B and OCT2 at almost all investigated concentrations, while cells expressing CAT2A only showed a significant uptake at concentrations above 300 μM. Uptake of MATE1 overexpressing cells was significantly ($p < 0.05$) higher at pH 7.8 and 8.2 than controls. Apparent V_{max} values (nmol mg protein^{-1} min^{-1}) for cellular uptake of ADMA and L-arginine were $\approx$11.8 ± 1.2 and 19.5 ± 0.7 for CAT2A, $\approx$14.3 ± 1.0 and 15.3 ± 0.4 for CAT2B, and 6.3 ± 0.3 and >50 for OCT2, respectively. Apparent K_m values (μmol/l) for cellular uptake of ADMA and L-arginine were $\approx$3,033 ± 675 and 3,510 ± 419 for CAT2A, $\approx$4,021 ± 532 and 952 ± 92 for CAT2B, and 967 ± 143 and >10,000 for OCT2, respectively. ADMA and L-arginine are substrates of human CAT2A, CAT2B, OCT2 and MATE1. Transport kinetics of CAT2A, CAT2B, and OCT2 indicate a low affinity, high capacity transport, which may be relevant for renal and hepatic elimination of ADMA or L-arginine.

Keywords Asymmetric dimethylarginine · ADMA · L-Arginine · Cationic amino acid transporter 2 · Organic cation transporter 2 · Multidrug and toxin extrusion protein 1

Abbreviations

AGXT	Alanine-glyoxylate aminotransferase
ADMA	Asymmetric dimethylarginine
CAT	Cationic amino acid transporter
CI	Confidence interval
DDAH	Dimethylarginine dimethylaminohydrolase
HEK	Human embryonic kidney cells 293
HEPES	4-(2-Hydroxyethyl)-1-piperazineethanesulfonic acid
V_{max}	Maximum transport velocity
MATE	Multidrug and toxin extrusion protein
NO	Nitric oxide
NOS	Nitric oxide synthase
OCT	Organic cation transporter
MES	2-(*N*-morpholino)ethanesulfonic acid
MPP^+	1-Methyl-4-phenylpyridinium
PCR	Polymerase chain reaction
SDS	Sodium dodecyl sulfate
TBS	Tris-buffered saline
y^+LAT	y^+L amino acid transporters

Introduction

Asymmetric dimethylarginine (ADMA) is an inhibitor of nitric oxide (NO) synthases and inhibits the synthesis of

J. Strobel · F. Müller · O. Zolk · B. Endreß · J. König · M. F. Fromm · R. Maas (✉)
Emil Fischer Center, Institute of Experimental and Clinical Pharmacology and Toxicology, Friedrich-Alexander-Universität Erlangen-Nürnberg, Fahrstraße 17, 91054 Erlangen, Germany
e-mail: renke.maas@pharmakologie.med.uni-erlangen.de

NO from L-arginine (Vallance et al. 1992). It is endogenously formed in cells by asymmetric dimethylation of L-arginine moieties of proteins followed by protein degradation and liberation of ADMA (Tang et al. 2000). Infusion of ADMA has been shown to impair endothelium-dependent relaxation and to increase blood pressure in humans (Achan et al. 2003; Vallance et al. 1992; Kielstein et al. 2004). Elevated plasma concentrations (frequently observed in patients suffering from end-stage renal disease), have been linked to cardiovascular disease and death (Böger et al. 2009; Zoccali et al. 2001).

Intracellular ADMA is primarily converted to L-citrulline and dimethylamine (DMA) by dimethylarginine dimethylaminohydrolase(s) (DDAHs) and to α-keto-δ-(*N*,*N*-dimethylguanidino)valeric acid (DMGV) by alanine-glyoxylate aminotransferase 2 (AGXT2) (Vallance and Leiper 2004; Rodionov et al. 2010). In vivo ADMA appears to be exchanged between net generation and net metabolizing tissues via transmembrane transport systems (Strobel et al. 2012). The liver (Siroen et al. 2005) and the kidneys (Nijveldt et al. 2002) are the major ADMA clearing organs in healthy humans due to a high expression of DDAH and AGXT2. Uptake or efflux transporter function, which is required by positively charged ADMA to pass cellular membranes, may be modified by endogenous or xenobiotic substances or as a functional consequence of genetic variations and may affect elimination and plasma concentrations of ADMA. Therefore, transport of ADMA is viewed as a potential therapeutic target to alter pathophysiological effects of ADMA.

Recently, we could show that the cationic amino acid transporter 1 (CAT1, *SLC7A1*), which is the most prominent transporter for L-arginine and ubiquitously expressed with exception of the liver (Closs et al. 1997b, 2006), mediates cellular uptake and export of ADMA (Strobel et al. 2012). However, with the exception of system y^+L amino acid transporters (y^+LAT) (Closs et al. 2012), alternative transport mechanisms remain elusive, especially in the liver. Considering the cation charge and the structural similarities of L-arginine and ADMA, carriers such as CAT1, CAT2A (*SLC7A2A*) and CAT2B (*SLC7A2B*), which belong to the same subfamily of solute carriers, are promising candidates (Closs et al. 1997a, b, 2006). Although CAT2A and CAT2B are splice variants and only differ in a stretch of 42 amino acids, they have distinct transport properties and expression patterns (Closs et al. 1997b; Kavanaugh et al. 1994). CAT2A shows a 10- to 30-fold lower substrate affinity to cationic amino acids, a greater maximal transport velocity and relative insensitivity to trans-stimulation as compared to CAT1 and CAT2B, which are classified with the y^+ system (Kavanaugh et al. 1994; Closs et al. 1997b). The CAT2A expression is high in the liver and weak in the skeletal muscle and pancreas, while CAT2B can be induced by pro-inflammatory cytokines and bacterial polysaccharide in a variety of cells including T cells, macrophages, lung, and testis (Closs et al. 2006; Mann et al. 2003). Further potential candidates for ADMA transport are the human organic cation transporter 2 (OCT2; *SLC22A2*) and the human multidrug and toxin extrusion protein 1 (MATE1). Uptake of ADMA by CAT2A, CAT2B, OCT2, and MATE1 has not been investigated, yet.

The OCT2 is localized to the basal membrane of renal proximal tubular cells and in neurons (Koepsell et al. 2007). It plays an important role in renal secretion of small and structurally diverse organic cations, including several drugs (Pietig et al. 2001). This could make it a possible target for drug interactions with ADMA elimination. Transport by OCT2 is bidirectional, independent of pH or sodium, and its affinity for certain substrates depends on their degree of ionization (Barendt and Wright 2002; Winter et al. 2011). MATE1 is a proton-substrate antiporter expressed both in the luminal membrane of renal tubules and in the canalicular membrane of hepatocytes (Otsuka et al. 2005). Export of cations into both urine and bile are mediated by MATE1, and its transport is enhanced by an oppositely directed proton gradient (Tsuda et al. 2007). Several substrates of MATE1 are also substrates of OCT2 (e.g., agmatine and metformin (Winter et al. 2011; Zolk et al. 2009), which show some structural similarity to L-arginine and ADMA). Therefore, it has been proposed that the coordinate activity of OCT2-mediated uptake from the blood and export into the urine by MATE1 is responsible for renal tubular secretion (Meyer zu Schwabedissen et al. 2010; König et al. 2011). The molecular mechanism of renal tubular secretion of ADMA is still unknown, but OCT2 and MATE1 are promising candidates.

The aim of this study was to investigate the cellular transport properties of new candidate transporters (CAT2A, CAT2B, OCT2, MATE1) that may be involved in transport of ADMA.

Materials and methods

Chemicals

^{3}H-labelled L-arginine (43 Ci/mmol), ^{3}H-labelled 1-methyl-4-phenylpyridinium (MPP^+, 80 Ci/mmol), and ^{14}C-labelled metformin (30 mCi/mmol) were purchased from American Radiolabelled Chemicals, Inc (St. Louis, MO, USA). ^{3}H-labelled ADMA (25 Ci/mmol) was obtained from BIOTREND Chemikalien GmbH (Cologne, Germany). Unlabelled L-arginine and ADMA were purchased from Enzo Life Sciences GmbH (Lörrach,

Germany). Sodium butyrate was obtained from Merck KGaA (Darmstadt, Germany).

Unlabelled MPP^+-iodide, metformin, and poly-D-lysine hydrobromide were purchased from Sigma-Aldrich Chemie GmbH (Taufkirchen, Germany). All other chemicals and reagents, unless stated otherwise, were purchased from Carl Roth GmbH & Co. KG (Karlsruhe, Germany) and were of the highest grade available. Stock solutions of ^{3}H-labelled ADMA and L-arginine in water contained 50 and 2 % ethanol, respectively. ^{3}H-labelled metformin and MPP-iodide were dissolved in ethanol. Final ethanol concentrations were lower than 0.1 % in all experiments. Water was used as a solvent for all other substances.

Cell culture

As previously described (Strobel et al. 2012), human embryonic kidney cells 293 (HEK) were cultured in minimal essential medium containing 10 % heat-inactivated fetal bovine serum, 100-U/ml penicillin, and 100-µg/ml streptomycin at 37 °C and 5 % CO_2. The cells were routinely subcultured by trypsinization using trypsin (0.05 %)-EDTA (0.02 %) solution. Culture media supplements for all cells were purchased from Invitrogen GmbH (Karlsruhe, Germany). HEK293 cells lines transfected with human OCT2 (HEK-OCT2) (Zolk et al. 2009) and human MATE1 (HEK-MATE1) (Müller et al. 2011) were previously established and characterized.

Generation of HEK293 cell lines stably overexpressing human CAT2A or CAT2B

A real-time PCR-based approach using hepatic (for *SCL7A2A*) or renal (for *SLC7A2B*) mRNA and the IScript cDNA Synthesis kit for sscDNA synthesis (Bio-Rad Laboratories GmbH, Munich, Germany) were used to clone *SLC7A2A* and *SLC7A2B* cDNA encoding human CAT2A and CAT2B, respectively.

The cDNA templates were amplified by polymerase chain reaction (PCR) using the GoTaq™ Hot Start Polymerase Kit (Promega GmbH, Mannheim, Germany) and the following primers: hCAT2A: forward 5′-CCACGAAA CTAGCAACTGGA-3′; reverse 5′-AGCTCTGCTCCTGC AAGTGT-3′; hCAT2B: forward 5′-AGACGTCAGAATG ATTCCTTGCA-3′; reverse 5′-CCAGCTCTGCTCCTGC AAGT-3′. An initial denaturation step of 2 min at 95 °C was followed by 45 cycles of denaturation at 95 °C for 30 s, annealing for 30 s at 56 °C for CAT2A or at 66 °C for CAT2B, and extending for 2 min at 72 °C. The corresponding cDNA was cloned into the pCR2.1-TOPO vector and subsequently subcloned into the pcDNA3.1/Hygro (−) vector (Invitrogen GmbH). Single nucleotide variations identified by sequencing and comparison to the NM_003046.5 (CAT2A) and NM_001008539.3 (CAT2B) sequences were corrected using the QuikChange™ Multi Site-Directed Mutagenesis Kit (Agilent Technologies Deutschland GmbH, Waldbronn, Germany), respectively. Using the Effectene™ Transfection Reagent Kit (QIAGEN GmbH, Hilden, Germany) HEK293 cells were transfected with the expression vector containing the *SLC7A2A* and *SLC7A2B* cDNAs, respectively. After hygromycin (250 µg/ml) treatment, single colonies (HEK-CAT2A and HEK-CAT2B, respectively) were selected and characterized for mRNA, CAT2 protein expression and CAT2 protein localization by quantitative real-time PCR, immunoblot analysis, and immunofluorescence, respectively. The same method but using the empty expression vector for transfection was performed to establish HEK-VC.

Real-time PCR

Quantitative real-time PCR using the LightCycler 2 System (Roche Diagnostics-Applied Science, Mannheim, Germany) was used to measure *SLC7A2A* and *SLC7A2B* mRNA, respectively. mRNA concentrations (expressed as arbitrary units) were normalized to the housekeeping gene β-actin. PCR was performed using Light Cycler FastStart DNA MasterPLUS SYBR Green I reagents (Roche Diagnostics-Applied Science) and the following primers: hCAT2A (forward 5′-GCCCGGGATGGCTTACTGTT-3′ and reverse 5′-GCATGGTGACCTGGGACTCA-3′, amplicon size of 301 base pairs), hCAT2B (forward 5′-CTATG GCGGAGGATGGGTTG-3′ and reverse 5′-GCATGGTGA CCTGGGACTCA-3′, amplicon size of 309 base pairs), and β-actin (forward 5′-TGACGGGGTCACCCACACTGTGC CCATCTA-3′ and reverse 5′-CTAGAAGCATTTGCGGT GGACGATGGAGGG-3′, amplicon size of 661 base pairs). Amplification of PCR fragments was performed with an initial denaturation step of 10 min at 95 °C, followed by 40 cycles of denaturation at 95 °C for 10 s, annealing for 10 s at 64 °C, and extending for 30 s at 72 °C. A melting curve and agarose gel analysis was performed after DNA amplification.

Immunoblot analysis

HEK-CAT2A, HEK-CAT2B, or HEK-VC cells were seeded in poly-D-lysine-coated cell culture plates (diameter 10 cm) at an initial density of 3.0×10^6 cells/plate. Cells were incubated for 24 h at 37 °C and 5 % CO_2 and treated with 10-mmol/l sodium butyrate for further 24 h to obtain higher levels of the recombinant protein (Cui et al. 1999). After centrifugation, each cell pellet was resuspended in 0.2 % sodium dodecyl sulfate (SDS) containing protease inhibitors (mini-complete protease inhibitor cocktail tablets; Roche Diagnostics-Applied Science). The bicinchoninic

acid assay (BCA Protein Assay Reagent, Thermo Fisher Scientific Inc, Rockford, IL, USA) was used to measure protein concentrations. 20 µg of total protein was diluted with Laemmli buffer (62 mmol/l Tris-HCl, 2 % SDS, 10 % glycerol, 0.01 % bromphenol blue, and 0.4 mmol/l dithiothreitol) and incubated at 95 °C for 5 min before fractionation on 10 % SDS-polyacrylamide gels. The protein molecular weight ranges were estimated by the BenchMark PreStained Protein Ladder (Invitrogen GmbH). The protein was transferred onto a nitrocellulose membrane (PROTRAN; Whatman Schleicher and Schuell, Dassel, Germany) using a tank blotting system (Bio-Rad Laboratories, Munich, Germany). Tris-buffered saline (TBS) containing 0.1 % Tween-20 (Sigma-Aldrich Chemie GmbH) and 5 % non-fat milk powder was used for blocking and served as matrix for the antibodies. Polyclonal rabbit anti-human CAT2 (1:333, HPA009169, Sigma-Aldrich Chemie GmbH) and monoclonal mouse anti-human β-actin (1:10,000, A5441, Sigma-Aldrich Chemie GmbH) were used as primary antibodies, and horseradish peroxidase-labelled goat anti-rabbit Fab fragments (1:1,000, Dianova, Hamburg, Germany) and peroxidase-affinipure goat anti-mouse IgG H+L (1:1,000, 115-035-003, Jackson ImmunoResearch Europe Ltd, Newmarket, Suffolk, UK) were used as secondary antibodies. HEK-VC cells served as controls. Protein detection was performed by ECL Western blotting detection reagents (GE Healthcare UK Ltd., Little Chalfont, UK) and digitally quantified using ChemiDoc XRS detection system (Bio-Rad Laboratories GmbH).

Immunofluorescence microscopy

Immunofluorescence staining and confocal microscopy using the Axiovert 100 M microscope (Carl Zeiss GmbH, Jena, Germany) and the Zeiss LSM Image Browser version 4.2.0.121 were used to analyze cellular localization of the CAT2 protein. HEK-CAT2A, HEK-CAT2B, and HEK-VC cells were seeded on object slides placed in cell culture plates at an initial density of 1×10^6 cells/slide, respectively. Cells were incubated for 24 h and treated with 10-mmol/l sodium butyrate for another 24 h. The human CAT2 antibody (1:100 in phosphate-buffered saline containing 1 % bovine serum albumine (Sigma-Aldrich Chemie GmbH) served as primary antibody, followed by the Alexa Fluor 488 conjugated secondary antibody (1:2,000, Molecular Probes, Eugene, OR, USA). Nuclei were counterstained with Sytox orange (1:50,000, Invitrogen GmbH).

Uptake transport assays

HEK-OCT2 and HEK-MATE1 cells have been already characterized (Zolk et al. 2009; Müller et al. 2011). HEK-CAT2A, HEK-CAT2B, HEK-OCT2, HEK-MATE1, or HEK-VC cells were seeded into poly-D-lysine-coated 24-well plates at an initial density of 3.5×10^5 cells/well. After 24 h, 10-mmol/l sodium butyrate was added for additional 24 h to induce CAT2A, CAT2B, OCT2, or MATE1 protein expression. For experiments investigating the pH-dependent MATE1-mediated uptake, transport buffers from pH 6.5–8.2 were used (142 mmol/l NaCl, 5 mmol/l KCl, 1 mmol/l K_2HPO_4, 1.2 mmol/l $MgSO_4$, 1.5 mmol/l $CaCl_2$, 5 mmol/l glucose, and either 12.5 mmol/l 4-(2-hydroxyethyl)-1-piperazineethanesulfonic acid (HEPES; for pH 6.9, 7.3, 7.8, and 8.2) or 2-(*N*-morpholino)ethanesulfonic acid (MES; for pH 6.5). All other experiments were performed with transport buffer pH 7.3. After washing with transport buffer (37 °C), the cells were incubated with a mixture of radiolabelled and nonradiolabelled L-arginine, ADMA, metformin, or MPP^+ in transport buffer at 37 °C. The period of linear uptake by CAT2A, CAT2B, or OCT2 was recognized by time dependence experiments. Therefore, cells were incubated with the transport buffer (containing 1,000 µmol/l ADMA and L-arginine, respectively) at 37 °C for 1, 2.5, 5, 10, and 30 min. For all experiments, the uptake period of 2.5 min was selected, because the CAT2A-, CAT2B-, or OCT2-based net uptakes of ADMA or L-arginine were all linear over 5 min (ADMA: CAT2A, $R^2 = 0.999$; CAT2B, $R^2 = 0.997$; OCT2, $R^2 = 0.969$. L-Arginine: CAT2A, $R^2 = 0.968$; CAT2B $R^2 = 0.970$; OCT2, $R^2 = 1.000$).

To determine the kinetic parameters of cellular uptake of ADMA and L-arginine by CAT2A, CAT2B, and OCT2, rising concentrations of up to 10 mmol/l for ADMA and 40 mmol/l for L-arginine were used. The selected incubation period of uptake of ADMA and L-arginine was 2.5 min for CAT2A, CAT2B, and OCT2 and 5 min for MATE1 [commonly used for various MATE1 substrates (Meyer zu Schwabedissen et al. 2010; Ohta et al. 2009)]. To verify OCT2 and MATE1 overexpression, uptake experiments with the prototypic substrates MPP^+ or metformin were performed. Subsequently, the cells were cooled to 0 °C, washed three times with ice-cold transport buffer and lysed with 0.2 % SDS. After addition of 4 ml of scintillation solution (Ultima Gold XR; PerkinElmer Life and Analytical Sciences, Inc., Rodgau-Jügesheim, Germany), the intracellular accumulation of radioactivity was determined by liquid scintillation counting (TriCarb 2800; PerkinElmer Life and Analytical Sciences, Inc.). The bicinchoninic acid assay was used to measure the appropriate protein concentration in each well. Data to calculate kinetic parameters were pooled from at least two single experiments each performed at least in triplicate ($n \geq 2 \times 3$) on different days.

Statistical analysis

As previously described (Strobel et al. 2012), net transport data were obtained by subtracting the uptake in cells transfected with the empty control vector from the uptake in cells transfected with *SLC7A2A*, *SLC7A2B*, *SLC22A2*, or *SLC47A1*. Hence, the maximum transport velocity (V_{max}) values have to be interpreted as "apparent" values. Michaelis–Menten enzyme kinetics in GraphPad Prism (version 5.01, 2007, GraphPad Software, San Diego, CA, USA) was used to calculate K_m values for the respective uptake transport. Each kinetic experiment was performed at least in triplicate, i.e. $n \geq 3$ wells per cell line and per investigated concentration. Data of at least two single kinetic experiments were pooled for K_m calculation. All data are presented as mean ± SEM. Unless stated otherwise, an unpaired, two-tailed t test was used to analyze differences in net uptake and CAT2 mRNA expression. A p value <0.05 was considered statistically significant.

Results

Generation of HEK293 cell lines stably overexpressing human CAT2A or CAT2B

To explore the cellular uptake properties of ADMA and L-arginine, cell lines stably overexpressing CAT2A (HEK-CAT2A) or CAT2B (HEK-CAT2B) were established (Fig. 1). As compared to control cells transfected with the empty expression vector (HEK-VC), significantly ($p < 0.001$) higher mRNA amounts of *SLC7A2A* and *SLC7A2B* (normalized to β-actin) were verified in HEK-CAT2A (Fig. 1a) and in HEK-CAT2B (Fig. 1b), respectively. A higher CAT2 protein expression in HEK-CAT2A and HEK-CAT2B cells was confirmed by immunoblot analyses (Fig. 1c). A strong signal was detected in HEK-CAT2A at around 78 kDa and in HEK-CAT2B cells at around 76 kDa, similar as previously prescribed (Visigalli et al. 2007) and corresponding to the mass weight of the human protein of CAT2A (76 kDa) and CAT2B (72 kDa). Endogenously expressed CAT2 protein was also observed in the empty-vector control cells, but to a much lower extent (Fig. 1d). As expected, CAT2 signal was located preferentially in the cell membrane.

Characterization of cellular uptake of ADMA and L-arginine by human CAT2A and CAT2B

As compared to control cells, significantly higher ($p < 0.01$) uptake rates of ADMA and L-arginine were observed at concentrations above 300 µmol/l in HEK-CAT2A cells (L-arginine: 300–30,000 µmol/l; ADMA: 300–6,000 µmol/l) and at all investigated concentrations in HEK-CAT2B cells (L-arginine: 10–10,000 µmol/l; ADMA: 0.1–6,000 µmol/l) (Fig. 2a–d). The CAT2A- or CAT2B-based net uptake was used to calculate the K_m and V_{max} values. The net uptake curves in Fig. 2a, c indicate that the K_m and V_{max} values for ADMA (which were calculated from the available data that was technically limited to a maximal ADMA concentration of 6,000 µmol/l) should be cautiously interpreted as approximations. For CAT2A-mediated uptake of ADMA and L-arginine, the V_{max} values were 11.8 ± 1.2 and 19.5 ± 0.7 nmol per mg total protein per minute, respectively (Fig. 2a, b). The corresponding K_m values were 3,033 ± 675 µmol/l (ADMA) and 3,510 ± 419 µmol/l (L-arginine).

For CAT2B-mediated uptake of ADMA and L-arginine, V_{max} values of 14.3 ± 1.0 and 15.3 ± 0.4 nmol per mg total protein per minute were determined, respectively (Fig. 2c, d). K_m values were 4,021 ± 532 µmol/l for ADMA and 952 ± 92 µmol/l for L-arginine. At extracellular ADMA and L-arginine concentrations typically found in vivo (ADMA: 0.1–1.0 µmol/l; L-arginine: 30–300 µmol/l), uptake of ADMA and L-arginine in HEK-CAT2B was 1.13- to 1.35-fold and 1.49- to 2.61-fold higher than in control cells, respectively.

Characterization of OCT2-mediated uptake of ADMA and L-arginine

Functionality of overexpressed OCT2 was verified using the prototypic OCT2 model substrate MPP^+, for which a considerably higher cellular uptake activity was verified in OCT2-overexpressing cells (HEK-OCT2) as compared to control cells (Fig. 3a). At almost all investigated concentrations (ADMA: 0.01–10,000 except 1 and 100 µmol/l, $0.05 < p < 0.08$; L-arginine: 10–40,000 µmol/l except 100 µmol/l, $p = 0.08$), uptake of ADMA and L-arginine in HEK-OCT2 was significantly higher ($p < 0.05$) than in control cells, respectively (Fig. 3b, c). At extracellular ADMA and L-arginine concentrations within the physiological range (ADMA: 0.1–1.0 µmol/l; L-arginine: 100 µmol/l), uptake of ADMA and L-arginine in HEK-OCT2 was 1.24- to 1.38-fold and 1.14-fold higher than in control cells, respectively. The OCT2-mediated net uptake was used to calculate the V_{max} and K_m values, which were 6.3 ± 0.3 nmol per mg total protein per minute and 967 ± 143 µmol/l for ADMA, respectively (Fig. 3b). The OCT2-mediated L-arginine uptake was not saturable even at 40,000 µmol/l (Fig. 3c). Thus, the V_{max} and K_m values could not be calculated but can be assumed to be at least higher than 50 nmol per mg total protein per minute and 10,000 µmol/l, respectively. In comparison to uptake experiments performed at 0 °C, the net uptake was significantly higher ($p < 0.05$) at 37 °C confirming that the

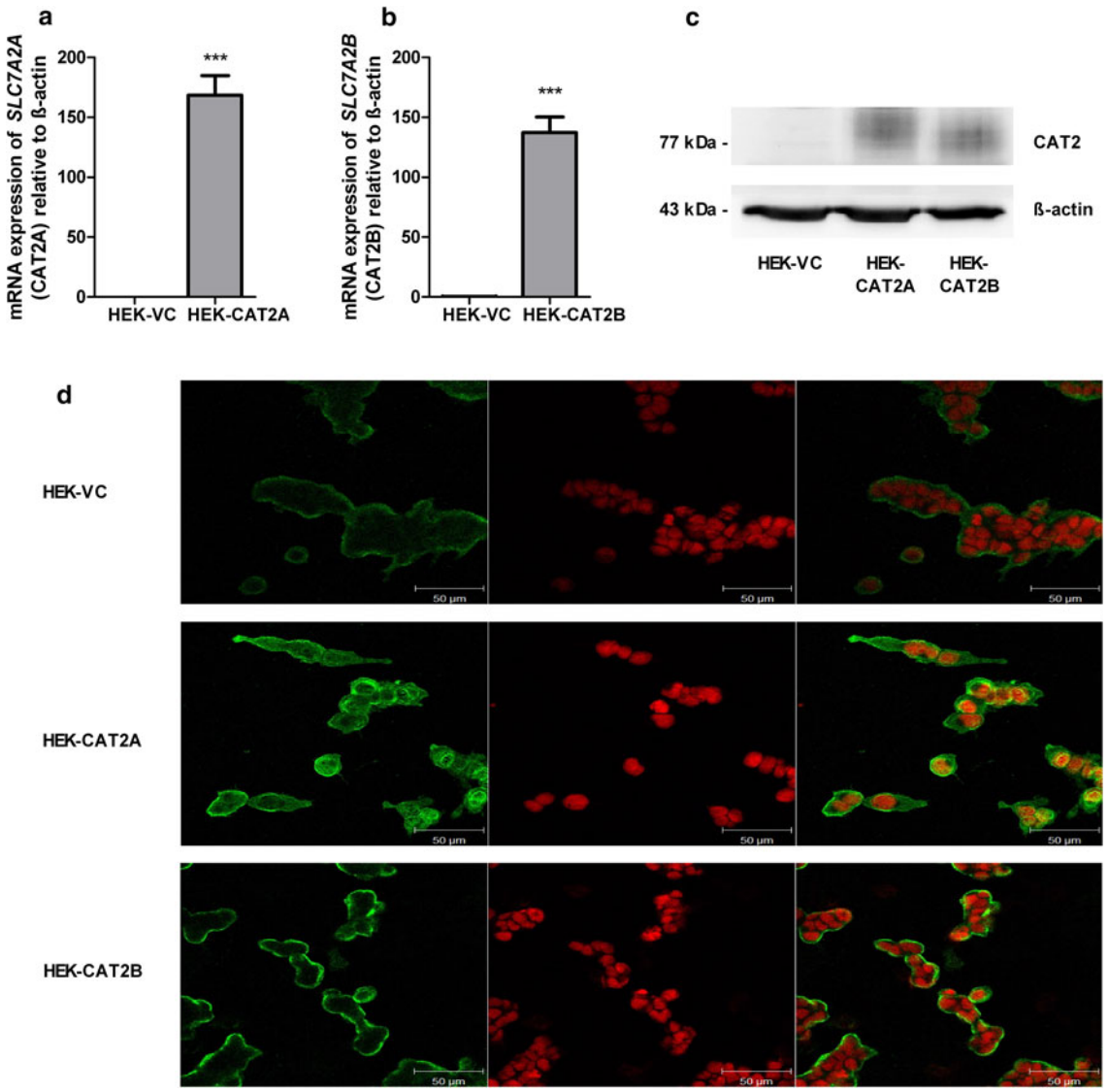

Fig. 1 Characterization of cell lines stably overexpressing human CAT2A (HEK-CAT2A) and human CAT2B (HEK-CAT2B). mRNA expression of **a** HEK-CAT2A and **b** HEK-CAT2B as compared to control cells transfected with the empty expression vector (HEK-VC). **c** Immunoblot analysis of human CAT2 protein in HEK-CAT2A, HEK-CAT2B, and HEK-VC (20 µg protein per lane were loaded). **d** Immunofluorescence analysis of human CAT2 protein in HEK-CAT2A, HEK-CAT2B, and HEK-VC. The CAT2 signal was preferably localized in the cell membrane and could also be detected in HEK-VC, but at a markedly lower content. CAT2 was visualized by confocal microscopy using a Alexa Fluor 488 conjugated secondary antibody (*green* fluorescence). The nuclei were counterstained *red*. ***$p < 0.001$, unpaired, two-tailed *t* test (color figure online)

observed uptake was indeed an active protein-mediated transport mechanism (Fig. 3d).

Investigation of MATE1-mediated cellular uptake of ADMA and L-arginine

The prototypic MATE1 model substrate metformin showed a significantly higher cellular uptake ($p < 0.001$) in HEK-MATE1 cells than in control cells (Fig. 4a), indicating functionality of the overexpressed MATE1. Equal uptake of ADMA (1 and 100 µmol/l) in HEK-MATE1 and control cells was observed at pH 6.5. With rising pH values, uptake in HEK-MATE1 cells increased and was significantly higher than in control cells at pH 7.3–8.2 ($p < 0.05$; Fig. 4b, c). At physiological L-arginine concentrations (100 µmol/l), a significantly higher uptake of L-arginine was seen in HEK-MATE1 cells at pH 6.5–8.2 ($p < 0.01$). At supraphysiological L-arginine concentrations (1,000 µmol/l), uptake in HEK-MATE1 was still significantly higher than in control cells at pH 7.8 and 8.2 ($p < 0.001$), but not at pH 6.5–7.3.

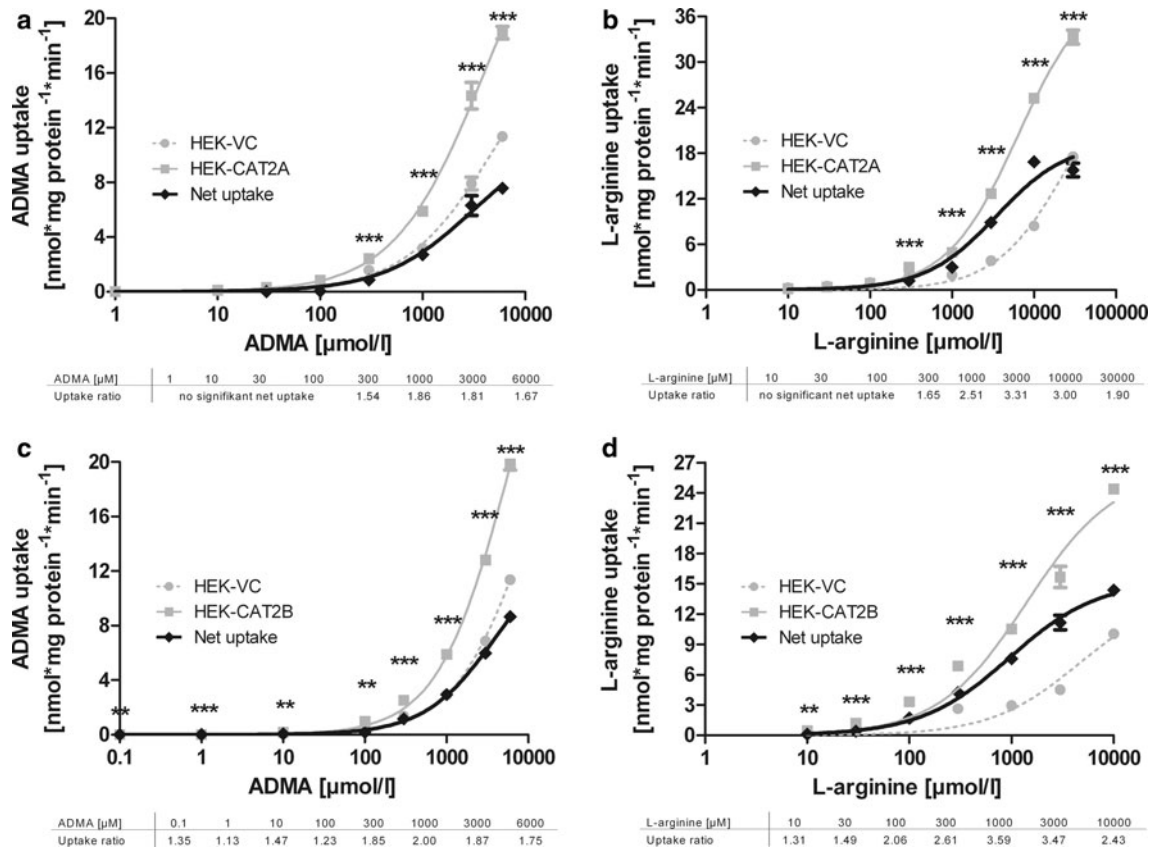

Fig. 2 Kinetics of CAT2A-mediated cellular uptake of **a** ADMA and **b** L-arginine and kinetics of CAT2B-mediated cellular uptake of **c** ADMA and **d** L-arginine. Cellular uptake of ADMA and L-arginine in cells stably overexpressing human CAT2A or CAT2B (HEK-CAT2A and HEK-CAT2B, respectively; *gray closed squares*) in comparison to control cells (HEK-VC, *gray closed circles*). The difference of uptake between overexpressing cells (HEK-CAT2A and HEK-CAT2B, respectively) and HEK-VC represents the CAT2A- or CAT2B-based net uptake (*black* rhombs). The uptake ratios of overexpressing cell lines (CAT2A and CAT2B, respectively) and the HEK-VC are shown in the tables below the kinetic graphs. Incubation periods for ADMA and L-arginine were 2.5 min. Uptake was standardized to the total protein amount. Experiments were performed at least in quadruplicate per day at two different days ($n \geq 2 \times 4$). $^{**}p < 0.01$, $^{***}p < 0.001$, unpaired, two-tailed *t* test

Discussion

In order to identify new transport pathways of ADMA and L-arginine and to assess their potential relevance, we used newly established HEK293 cells stably overexpressing CAT2A and CAT2B and already characterized HEK293 cells overexpressing OCT2 and MATE1. Radiolabelled ADMA and L-arginine were used as substrates to characterize and to compare transport kinetics. Our principal findings are:

1. ADMA and L-arginine are substrates of human CAT2A, CAT2B, OCT2, and MATE1.
2. Uptake kinetics of ADMA and L-arginine by CAT2A, CAT2B, and OCT2 suggest a low affinity and high capacity transport pattern.
3. Uptake of ADMA and L-arginine by MATE1 is pH-dependent.

By measuring the uptake of radiolabelled ADMA into HEK293 cells overexpressing human CAT2A, CAT2B, or OCT2, the first direct kinetic data for cellular uptake of ADMA by human CAT2A, CAT2B, and OCT2, respectively, were generated. In addition, kinetic data for L-arginine were determined to evaluate substrate-specific differences and as a positive control for comparison with published data. Previous studies investigating the uptake of L-arginine in native endothelial cells or macrophages were limited by the fact that these studies relied on endogenous expression of known and unknown membrane transporters and, thus, did not permit to assess the distinct kinetics of individual transporters (Diaz-Perez et al. 2012; Closs et al. 2000). High-affinity transport kinetics were mostly attributed to CAT1, but the possible contribution of lower affinity transporters resembling system y^+ or y^+L could not be further elucidated. Our findings regarding cellular uptake of L-arginine by human CAT2A (K_m value: 3,510 µmol/l) were in line with previous transport studies of murine and human CAT2A in the Xenopus laevis oocytes overexpression system (K_m values: 2,150–5,200 µmol/l (Closs et al. 1993)

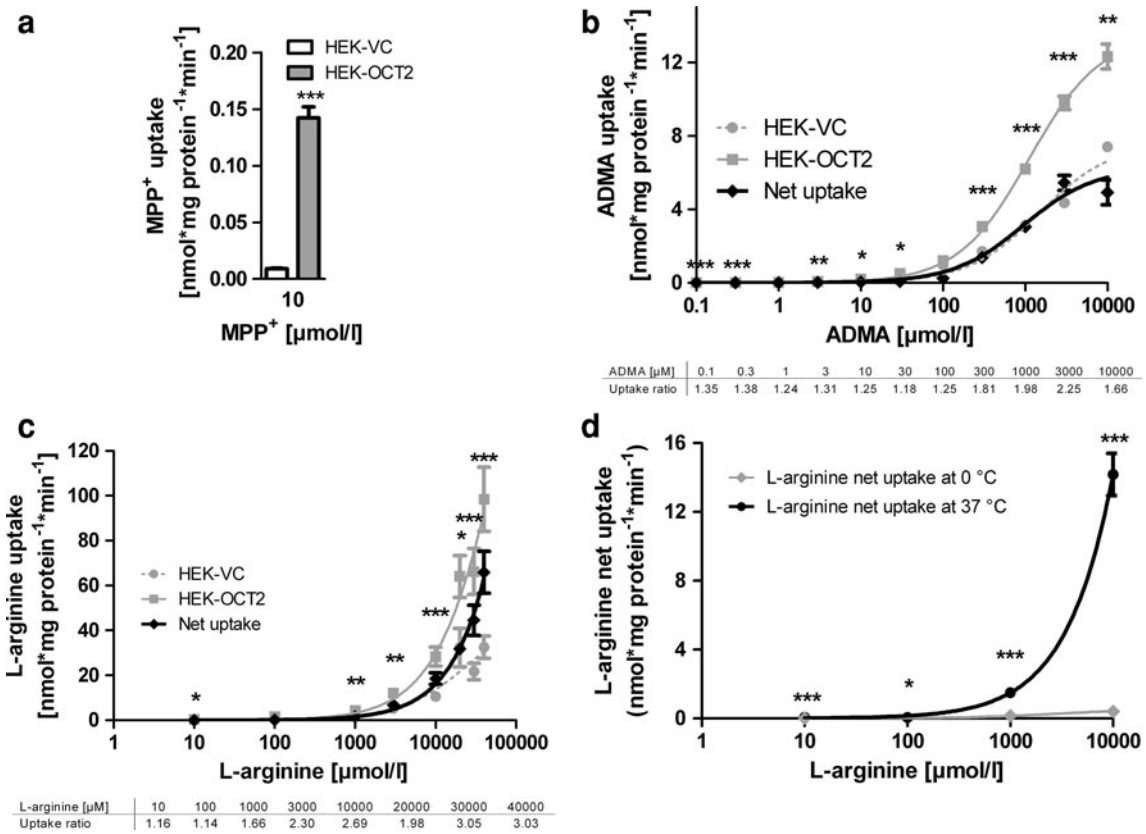

Fig. 3 Kinetics of OCT2-mediated cellular uptake of ADMA and L-arginine. **a** Control uptake of the OCT2 model substrate MPP^+ (10 µmol/l; incubation period: 10 min; $n = 3$). **b** Cellular uptake of ADMA and **c** L-arginine by OCT2 overexpressing cells (HEK-OCT2, *gray closed squares*) and control cells (HEK-VC, *gray closed circles*). The difference between overexpressing cells and HEK-VC represents the OCT2-based net uptake (*black* rhombs) and was used to calculate the maximum transport velocity (V_{max}) and K_m value. The K_m value represents the substrate concentration at half maximum transport velocity. The uptake ratios of OCT2 overexpressing cells (HEK-OCT2) and HEK-VC are presented in the tables below the kinetic graphs. The incubation period for ADMA and L-arginine was 2.5 min. Uptake was standardized to the total protein amount. Experiments were performed at least in triplicate per day at two different days ($n \geq 2 \times 3$; except ADMA 10,000 µmol/l with $n = 3$ due to apparent cell impairment). **d** To confirm OCT2-mediated L-arginine transport, L-arginine (10–10,000 µM) uptake at 37 °C was compared to uptake measured at 0 °C ($n = 4$). $^*p < 0.05$, $^{**}p < 0.01$, $^{***}p < 0.001$, unpaired, two-tailed t test)

and 3,360–3,900 µmol/l (Closs et al. 1997b), respectively). Our K_m value for CAT2B-mediated uptake of L-arginine (K_m value: 915 µmol/l) was slightly higher as compared to previous transport kinetics studies of human and murine CAT2B in Xenopus laevis oocytes (K_m values: 320–730 µmol/l and 250–380 µmol/l (Closs et al. 1997b), respectively). However, these minor differences may be explained by differences in assay conditions from our cell system including the temperature (e.g., 19–20 °C vs. 37 °C). Nevertheless, the K_m value for L-arginine uptake was twice as high for CAT2B than for CAT1, which was in agreement with previous results (Closs et al. 1997b). Key measurements were performed with substrate concentrations of ADMA (1 µmol/l) and L-arginine (100 µmol/l) that can be observed in vivo (Vallance et al. 1992; Zoccali et al. 2001). Metabolism of intracellular ADMA or L-arginine and subsequent cellular export of their metabolites is negligible in the assay setting we used and unlikely to significantly affect our results during our incubation time of 2.5–5 min. In a pilot experiment, HEK293 cell homogenate was incubated with 10 µmol/l ^{2}H-labelled ADMA for 60 min and only 0.2 % of added ^{2}H-labelled ADMA was degraded per minute.

Physiological intracellular concentrations of both ADMA and L-arginine exceed plasma concentrations and may alter cellular uptake kinetics by trans-stimulation. Based on bovine and rat endothelial cells, intracellular concentrations amount to 4–12 µmol/l for ADMA and 100–800 µmol/l for L-arginine (Teerlink et al. 2009; Baydoun et al. 1990). In HEK293 cells, we measured ($N = 18$) intracellular concentrations of 0.092 ± 0.006 nmol mg protein^{-1} for ADMA and 3.084 ± 0.404 nmol mg protein^{-1} for L-arginine giving an L-arginine/ADMA ratio of 33.4 ± 3.4. Based on a "volume" of 6.5 µl mg protein^{-1} as calculated for HEK293 cells (Mateus et al. 2013) this corresponds to cellular concentrations of 14.2 and

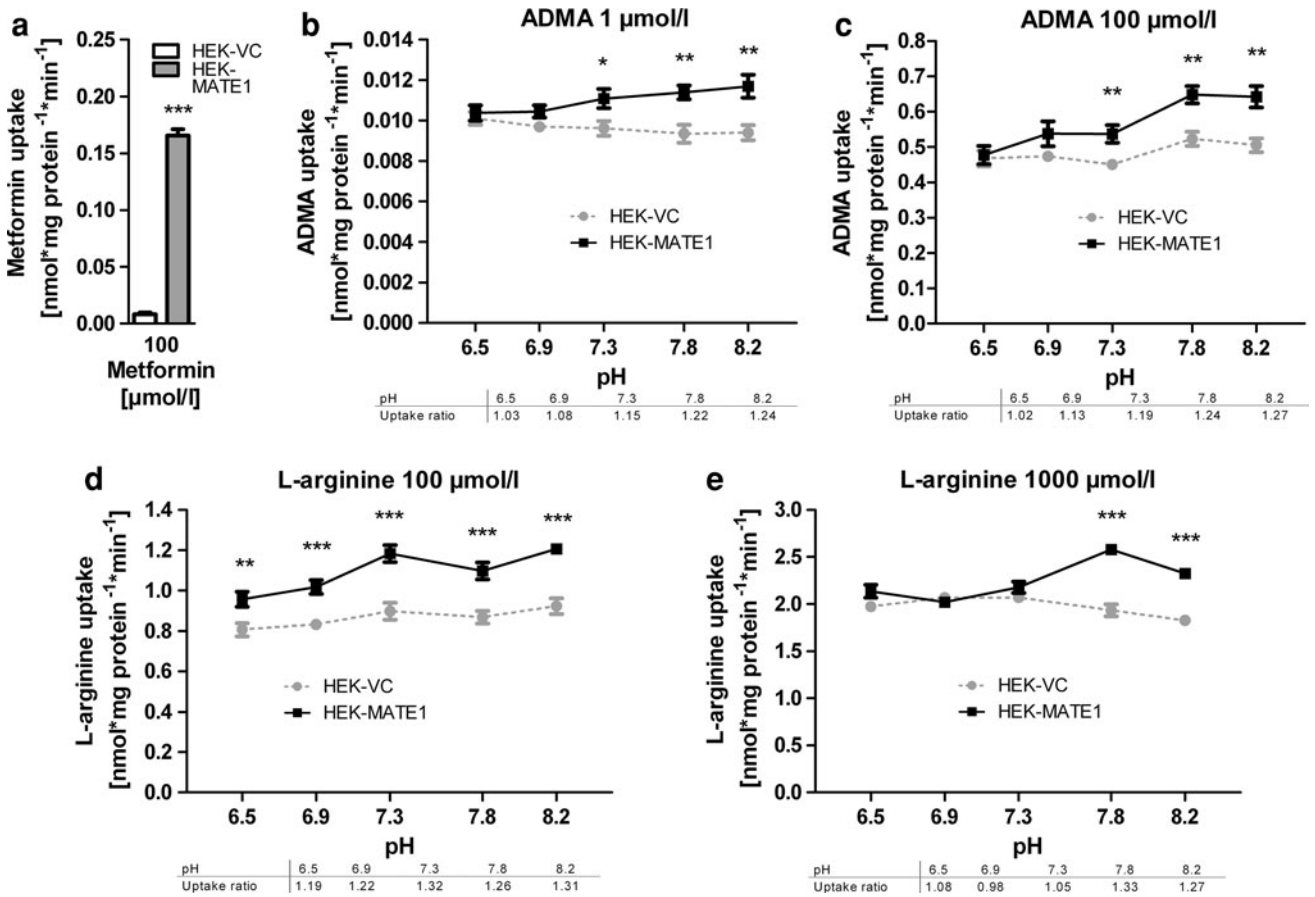

Fig. 4 MATE1-mediated uptake of ADMA and L-arginine. **a** Control uptake of the MATE1 model substrate metformin (100 µmol/l; incubation period: 5 min; extracellular pH: 7.8). Cellular uptake of **b** 1 µmol/l ADMA, **c** 100 µmol/l ADMA, **d** 100 µmol/l L-arginine, and **e** 1,000 µmol/l L-arginine by MATE1 overexpressing cells (HEK-MATE1, *black closed squares*) and control cells (HEK-VC, *gray closed circles*). pH dependence was investigated from pH 6.5–8.2. The incubation period was 5 min for metformin, ADMA, and L-arginine. The uptake ratios of MATE1 overexpressing cells (HEK-MATE1) and HEK-VC are shown in the tables below the *graphs*. Uptake was standardized to the total protein amount. Experiments were performed at least in quadruplicate per day at two different days ($n \geq 2 \times 4$). $^{*}p < 0.05$, $^{**}p < 0.01$, $^{***}p < 0.001$, unpaired, two-tailed *t* test)

474 µmol/l for ADMA and L-arginine, respectively, which is similar to the published data (Teerlink et al. 2009).

ADMA is a substrate of human CAT2A

Increased cellular uptake of the nitric oxide synthase (NOS) inhibitor ADMA or the decreased uptake of the NOS substrate L-arginine may lead to decreased NO production and related adverse consequences for cardiovascular health (Teerlink et al. 2009). Here, we showed that ADMA is a substrate for human CAT2A. Kinetics of CAT2A-mediated cellular uptake of ADMA and L-arginine were consistent with a low affinity (K_m values >3,000 µmol/l) and high capacity transport, with a 1.7-fold higher transport capacity (V_{max}) for L-arginine than for ADMA. Of note, significant CAT2A-mediated uptake of both ADMA and L-arginine was detected only at high ADMA and L-arginine concentrations and not at concentrations, as low as the plasma levels generally found in humans. Thus, these data suggest that CAT2A plays a less important role in ADMA transport than CAT1, which exhibits a higher affinity to ADMA (>15-fold lower K_m value), a 2.3-fold higher transport capacity (Strobel et al. 2012), and a less restricted expression pattern (ubiquitously expressed with exception of the liver) than CAT2A (Closs et al. 2006; Mann et al. 2003). This may explain the observation that mice tolerate the knockout of CAT2A quite well (Nicholson et al. 2001), whereas genetic ablation of CAT1 is lethal (Perkins et al. 1997). Furthermore, ADMA plasma concentrations are very low (100–200 times lower compared to L-arginine) and only show a slightly higher transport affinity to CAT2A than L-arginine (1.16-fold smaller K_m value) to relevantly displace/inhibit L-arginine. Assuming the L-arginine plasma concentration typically in the range of 50–100 µmol/l, only 5–10 % of CAT2A is occupied by L-arginine (Closs et al. 1993). Taken together these data indicate that ADMA is

unlikely to competitively inhibit CAT2A-mediated transport of L-arginine under physiological conditions.

ADMA is a substrate of human CAT2B

CAT1 and CAT2B are known uptake transport proteins for cationic amino acids such as L-arginine and L-lysine and show similar transport properties illustrating the y^+ system (e.g., high affinity, sodium-independent, and bidirectional transport showing a sensitive stimulation by substrates at the trans-side of the membrane) (Closs et al. 1997b). The results of the present study show that ADMA is also transported by CAT2B. However, despite the high overexpression of CAT2B (>700-fold higher *SLC7A2B* mRNA amount uptake was just 10–50 % higher than in control cells at concentrations within or close to the physiological range (0.1, 1, and 10 µmol/l). In addition, we observed a distinctly reduced affinity and reduced transport capacity of CAT2B to ADMA (20 times higher K_m and halved V_{max} value) as compared to CAT1 (Strobel et al. 2012). Therefore, these data show that ADMA is transported by human CAT2B, but at a considerably lower extent as compared to the almost ubiquitously expressed CAT1.

At physiological concentrations, uptake of L-arginine (uptake ratio at 100 µmol/l: 2.06) clearly exceeded that of ADMA (uptake ratio at 1 µmol/l: 1.13). Therefore, a higher activity/expression of CAT2B may lead to an increased uptake of the NOS substrate L-arginine, while the uptake of the NOS inhibitor ADMA is relatively smaller. As a consequence, CAT2B (especially when upregulated) may enhance NOS activity.

However, we postulate that ADMA at physiological levels is unlikely to competitively impair CAT2B-mediated uptake of L-arginine, because its affinity to CAT2B is four times lower and the plasma concentrations are 100–200 times lower as compared to L-arginine. Still, these data are largely in line with a study by Closs et al., who reported an inhibition of CAT2B-mediated uptake of 50 µmol/l L-arginine by 250–10,000 µmol/l ADMA in Xenopus laevis oocytes (Closs et al. 1997a). In that study, ADMA concentrations were at least 100–1,000 times higher than those found in vivo and exceeded the L-arginine concentrations at least by the factor 5–10. Nevertheless, only 20 and 47 % of L-arginine uptake was inhibited by 250 and 500 µmol/l ADMA. Hence, it can be assumed that much lower ADMA concentrations are unlikely to have a physiologically relevant effect on CAT2B-mediated uptake of L-arginine.

ADMA and L-arginine are substrates of human OCT2

In the present study, human OCT2 was identified as a new transport protein involved in cellular uptake of ADMA and L-arginine. Both substrates show a low affinity to OCT2 (high K_m values >900 µmol/l), but distinct transport capacities. While transport capacity was very high and not saturable for L-arginine uptake, it was rather low for ADMA (V_{max} values: >50 versus 6.3 nmol/mg total protein per minute, for L-arginine and ADMA, respectively; see Table 1). At physiological extracellular concentrations of ADMA and L-arginine, uptake of both ADMA and L-arginine was only marginally higher in OCT2 overexpressing cells than in controls (1.2- to 1.4-fold higher uptake for 0.1–1.0 µmol/l ADMA and 1.1- to 1.2-fold higher uptake for 10–100 µmol/l L-arginine). This suggests that OCT2 may be more involved in cellular uptake of surplus L-arginine (≥300 µmol/l), while it may contribute (albeit not dominantly) to ADMA uptake at physiological concentrations.

ADMA and L-arginine are substrates of human MATE1

We identified ADMA and L-arginine as substrates of the efflux transporter MATE1, which is expressed at the luminal membrane of proximal renal tubules or canalicular membranes of hepatocytes (Otsuka et al. 2005). MATE1 may act as an uptake or export transporter depending on the direction of the transmembrane proton gradient (Tsuda et al. 2007). Acidification of the extracellular environment improves the export function of MATE1, while extracellular alkalinization or intracellular acidification increases the uptake of substrates (König et al. 2011; Meyer zu Schwabedissen et al. 2010; Otsuka et al. 2005). As expected, we observed an increasing MATE1-mediated uptake of ADMA and L-arginine at a rising alkaline extracellular environment, which confirmed the dependence of MATE1-based transport on the pH environment of the apical/extracellular compartment. This pattern was observed at both physiological and supraphysiological extracellular concentrations of ADMA or L-arginine, respectively. The low uptake ratios that were observed for MATE1-mediated transport indicate a low affinity of ADMA and L-arginine to MATE1, respectively. Interestingly, MATE1 is involved in a high-affinity export of agmatine, which is structurally similar to L-arginine and ADMA (K_m value: 8.6 ± 1.4 µmol/l; V_{max}: 64.3 ± 3.5 per mg total protein per minute) and could not be inhibited by 500 µmol/l L-arginine (Winter et al. 2011). Since both ADMA and L-arginine are substrates of MATE1, competitive inhibition is the expected mechanism. Thus, this may indicate that L-arginine exhibits a lower affinity to MATE1 than agmatine. Nevertheless, further investigation of transport kinetics of ADMA and L-arginine concerning MATE1 is reasonable. Another complementing export route of ADMA from non-epithelial cells by system y^+L amino acid transporters (y^+LAT) was previously demonstrated, where cells of a patient with severe coronary and

Table 1 Comparison of cellular uptake kinetics of ADMA and L-arginine

Substrate	ADMA		L-Arginine	
	K_m (μmol/l)	V_{max} (nmol mg protein^{-1} min^{-1})	K_m (μmol/l)	V_{max} (nmol mg protein^{-1} min^{-1})
CAT1, *SLC7A1* (Strobel et al. 2012)	183 ± 21	26.9 ± 0.8	519 ± 36	11.0 ± 0.2
CAT2A, *SLC7A2A*	≈3,033 ± 675[a]	≈11.8 ± 1.2[a]	3,510 ± 419	19.5 ± 0.7
CAT2B, *SLC7A2B*	≈4,021 ± 532[a]	≈14.3 ± 1.0[a]	952 ± 92	15.3 ± 0.4
OCT2, *SLC22A2*	967 ± 143	6.3 ± 0.3	>10,000 (estimate only)	>50 (estimate only)
MATE1, *SLC47A1*	Substrate (pH dependent)		Substrate (pH dependent)	

K_m and V_{max} values presented as mean ± SEM

[a] Calculation based on available data set

peripheral endothelial dysfunction, increased platelet aggregation, and increased platelet-derived superoxide production showed reduced y^+LAT expression and an impaired cellular ADMA efflux (against neutral amino acids) (Closs et al. 2012). During oral L-arginine administration those conditions improved and previously normal plasma ADMA levels markedly increased demonstrating enhanced ADMA efflux from intracellular stores. This suggests that y^+LAT plays an important role in depletion of surplus intracellular ADMA, which may lead to NOS inhibition and endothelial dysfunction.

Implications on cellular uptake mechanisms involving L-arginine and the "L-arginine paradox"

Considering intracellular L-arginine concentrations of 100–800 μmol/l (Teerlink et al. 2009; Baydoun et al. 1990, and the present estimate) and the half saturating L-arginine concentration for the endothelial NO synthase (K_m value) of 0.7–3.1 μmol/l (Cardounel et al. 2007; Hingorani 2001), the NO synthase is expected to be saturated at physiological intracellular concentrations of L-arginine. However, additional extracellular L-arginine was still found to stimulate intracellular NO synthase activity and this phenomenon was named the L-arginine paradox. High extracellular concentration of L-arginine was discussed to saturate the CAT system and either competitively inhibit cellular uptake or promote (by trans-stimulation) cellular export of ADMA (Tsikas et al. 2000; Teerlink et al. 2009). Hereby, the intracellular L-arginine/ADMA ratio, which is correlated with cellular NO production (Cardounel et al. 2007), may be altered in endothelial cells. We previously speculated that CAT1, the most prominent transporter for ADMA and L-arginine, may contribute to the L-arginine paradox, because its cellular uptake of ADMA can be inhibited at L-arginine concentrations in the physiological range (Strobel et al. 2012). In the current study, we continued the search for candidates involved in the L-arginine paradox and demonstrated that CAT2B may mediate uptake of ADMA. Considering a 100–200 times higher plasma concentration and a four times higher CAT2B affinity of L-arginine compared to ADMA, inhibition of CAT2B-mediated ADMA uptake by L-arginine may occur at physiological extracellular concentrations. However, due to the relatively small transport rate of CAT2B for ADMA (compared to CAT1), its inhibition is probably of minor relevance in vivo. Taken together, a contribution of the CAT 2B-mediated transport to the L-arginine paradox is possible, but likely to be small.

Implications for hepatic elimination of ADMA and L-arginine

The liver with its high expression of DDAH serves as a major clearing organ of circulating ADMA (Siroen et al. 2005). An increased urinary excretion and elevated plasma concentrations of ADMA were observed in patients with liver disease (Carnegie et al. 1977; Nickovic et al. 2012), and elevated ADMA levels were lowered after a successful liver transplantation (Siroen et al. 2004). CAT2A (but not CAT1) is highly expressed in the liver and was largely expected to similarly mediate ADMA uptake in a similar manner as known for L-arginine (Teerlink et al. 2009; Closs et al. 1993). However, the present data suggest that CAT2A (due to its high K_m value) is unlikely to be the primary uptake transport protein for ADMA in the liver. Still, the low affinity high capacity transport pattern of CAT2A may contribute to removal of surplus ADMA from the (portal) circulation. CAT2A features similar transport patterns for ADMA and L-arginine, since uptake only occurs at substrate concentrations that exceed the levels found in plasma (possible dietary excesses aside) (White and Christensen 1982; Closs et al. 1993). However, rats fed a diet of low salt for 7 days exhibited double *slc7a2a* mRNA expression in the liver (encoding CAT2A), raised plasma L-arginine concentrations and reduced plasma ornithine concentrations as well as the rate of urea generation (Kitiyakara et al. 2001). In an further publication, increased hepatic *slc7a2a*

mRNA and decreased plasma levels of ADMA and L-arginine were noticed in streptozotocin-induced diabetic rats versus controls, indicating an increased hepatic uptake of ADMA and L-arginine by overexpressed CAT2A in diabetic rats (Palm et al. 2008).

This indicates that despite the low affinity of ADMA and L-arginine, their uptake by CAT2A and their metabolism by the hepatic arginase–urea pathway (L-arginine) or by DDAH and AGXT2 (ADMA) may somehow affect NO production. However, our data suggest that the main transport mechanism for hepatic uptake of ADMA remains to be elucidated.

Implications for renal function and elimination of ADMA and L-arginine

Plasma levels of ADMA are particularly high in patients with chronic kidney disease (Vallance et al. 1992), but there are variable and conflicting findings whether reduced renal function contributes to this increase of ADMA in CKD (Fliser et al. 2005; Ronden et al. 2012). Cellular uptake of ADMA is essential for its degradation accomplished by intracellular renal DDAH or by secretion. In the current study, we found that CAT2B and OCT2 can mediate uptake of ADMA and L-arginine, while MATE1 can mediate their cellular efflux. The contribution of CAT2B and OCT2 to cellular ADMA uptake appears similar (with uptake ratios of 1.2–1.4 at physiological ADMA concentrations) but rather low. CAT2B and OCT2 may rather come into play when additional transport capacity is required to reduce the elevated plasma levels of ADMA (excess protein turnover or end-stage renal disease) or L-arginine (e.g., after enhanced L-arginine intake/supplementation) (Vallance et al. 1992; Dioguardi 2011). In contrast, CAT1 that shows a strong bidirectional and pH-independent ADMA transport (uptake ratios of 8.4–8.7) (Strobel et al. 2012; Closs et al. 2006) appears to be the dominant transport protein for cellular uptake of circulating ADMA in the kidney. According to our data, MATE1 is likely to be involved in renal secretion/elimination of ADMA into the urine, but also with a low transport rate (low uptake ratios at around 1.2). This suggests that MATE1 is involved in extrusion mechanisms to prevent rather surplus intracellular ADMA in the kidney; for instance, in patients with kidney diseases combined with overall elevated ADMA levels. In line with that, a significantly higher elimination of ADMA and L-arginine into the urine occurs in patients suffering from kidney diseases compared to healthy subjects (Carnegie et al. 1977). On the other hand, the low transport rates of MATE1 also indicate that secretion/loss of amino acids is restricted in healthy humans, because ADMA is usually recycled to L-citrulline (Vallance and Leiper 2004), which is a valuable amino acid and a key intermediate in the urea cycle (Bronk and Fisher 1956). Furthermore, the combination of OCT2 expressed in basal membrane of proximal tubular cells and the apically expressed MATE1, which was previously reported to determine vectorial secretion of cationic compounds across tubular epithelial cells (König et al. 2011), may also be relevant for elimination of ADMA and L-arginine. Hence, renal accumulation of inhibitors of OCT2 and MATE1 may influence this secretion and may provide a new target to regulate ADMA or L-arginine levels.

Moreover, uptake of ADMA and L-arginine into macula densa cells may also influence the renal function via the NOS-dependent tubular glomerular feedback pathway, which entails vasoconstriction of the afferent arteriole, a decrease of the glomerular capillary pressure and consequently a reduced glomerular filtration rate. Previous studies showed that inhibition of NOS (potentially by ADMA) reduced sodium chloride and fluid reabsorption from superficial proximal convoluted rat tubule (De Nicola et al. 1992). In addition, ADMA enhanced maximal tubular glomerular feedback responses when microperfused luminally into the macula densa (Tojo et al. 1997). Therefore, transport mechanisms by CAT1, CAT2B, OCT2, and MATE1 may also affect the renal function in general and not only the elimination of ADMA and L-arginine.

Conclusions

In summary, the present data demonstrate that CAT2A, CAT2B, and OCT2 contribute to the cellular uptake of ADMA and L-arginine, while MATE1 contributes to their cellular efflux. The extent of ADMA and L-arginine transport mediated by these transport proteins is likely to be inferior to the transport mediated by CAT1. However, the contribution of these transport proteins should be considered, in tissues not expressing CAT1 as well as in presence of highly elevated plasma or tissue concentrations of ADMA and L-arginine.

Acknowledgments This work was supported by an intramural grant of the Universität Erlangen-Nürnberg to Renke Maas and in part by a grant of the Deutsche Forschungsgemeinschaft (Fr1298/5-1) to Martin Fromm. Joachim Strobel is supported by a scholarship of the Friedrich-Ebert Foundation.

Conflict of interest The authors declare that they have no conflict of interest.

References

Achan V, Broadhead M, Malaki M, Whitley G, Leiper J, MacAllister R, Vallance P (2003) Asymmetric dimethylarginine causes

hypertension and cardiac dysfunction in humans and is actively metabolized by dimethylarginine dimethylaminohydrolase. Arterioscler Thromb Vasc Biol 23(8):1455–1459. doi:10.1161/01.ATV.0000081742.92006.59

Barendt WM, Wright SH (2002) The human organic cation transporter (hOCT2) recognizes the degree of substrate ionization. J Biol Chem 277(25):22491–22496. doi:10.1074/jbc.M203114200

Baydoun AR, Emery PW, Pearson JD, Mann GE (1990) Substrate-dependent regulation of intracellular amino acid concentrations in cultured bovine aortic endothelial cells. Biochem Biophys Res Commun 173(3):940–948. doi:10.1016/S0006-291X(05)80876-9

Böger RH, Sullivan LM, Schwedhelm E, Wang TJ, Maas R, Benjamin EJ, Schulze F, Xanthakis V, Benndorf RA, Vasan RS (2009) Plasma asymmetric dimethylarginine and incidence of cardiovascular disease and death in the community. Circulation 119(12):1592–1600. doi:10.1161/CIRCULATIONAHA.108.838268

Bronk JR, Fisher RB (1956) The role of ornithine and citrulline in urea synthesis. Biochem J 64(1):111–118

Cardounel AJ, Cui H, Samouilov A, Johnson W, Kearns P, Tsai AL, Berka V, Zweier JL (2007) Evidence for the pathophysiological role of endogenous methylarginines in regulation of endothelial NO production and vascular function. J Biol Chem 282(2):879–887. doi:10.1074/jbc.M603606200

Carnegie PR, Fellows FC, Symington GR (1977) Urinary excretion of methylarginine in human disease. Metabolism 26(5):531–537

Closs EI, Albritton LM, Kim JW, Cunningham JM (1993) Identification of a low affinity, high capacity transporter of cationic amino acids in mouse liver. J Biol Chem 268(10):7538–7544

Closs EI, Basha FZ, Habermeier A, Förstermann U (1997a) Interference of L-arginine analogues with L-arginine transport mediated by the y+ carrier hCAT-2B. Nitric Oxide 1(1):65–73. doi:10.1006/niox.1996.0106

Closs EI, Gräf P, Habermeier A, Cunningham JM, Förstermann U (1997b) Human cationic amino acid transporters hCAT-1, hCAT-2A, and hCAT-2B: three related carriers with distinct transport properties. Biochemistry 36(21):6462–6468. doi:10.1021/bi962829p

Closs EI, Scheld JS, Sharafi M, Förstermann U (2000) Substrate supply for nitric-oxide synthase in macrophages and endothelial cells: role of cationic amino acid transporters. Mol Pharmacol 57(1):68–74

Closs EI, Boissel JP, Habermeier A, Rotmann A (2006) Structure and function of cationic amino acid transporters (CATs). J Membr Biol 213(2):67–77. doi:10.1007/s00232-006-0875-7

Closs EI, Ostad MA, Simon A, Warnholtz A, Jabs A, Habermeier A, Daiber A, Förstermann U, Münzel T (2012) Impairment of the extrusion transporter for asymmetric dimethyl-L-arginine: a novel mechanism underlying vasospastic angina. Biochem Biophys Res Commun 423(2):218–223. doi:10.1016/j.bbrc.2012.05.044

Cui Y, König J, Buchholz JK, Spring H, Leier I, Keppler D (1999) Drug resistance and ATP-dependent conjugate transport mediated by the apical multidrug resistance protein, MRP2, permanently expressed in human and canine cells. Mol Pharmacol 55(5):929–937

De Nicola L, Blantz RC, Gabbai FB (1992) Nitric oxide and angiotensin II. Glomerular and tubular interaction in the rat. J Clin Invest 89(4):1248–1256. doi:10.1172/JCI115709

Diaz-Perez F, Radojkovic C, Aguilera V, Veas C, Gonzalez M, Lamperti L, Escudero C, Aguayo C (2012) L-Arginine transport and nitric oxide synthesis in human endothelial progenitor cells. J Cardiovasc Pharmacol 60(5):439–449. doi:10.1097/FJC.0b013e318269ae2f

Dioguardi FS (2011) To give or not to give? Lessons from the arginine paradox. J Nutrigenet Nutrigenomics 4(2):90–98

Fliser D, Kronenberg F, Kielstein JT, Morath C, Bode-Böger SM, Haller H, Ritz E (2005) Asymmetric dimethylarginine and progression of chronic kidney disease: the mild to moderate kidney disease study. J Am Soc Nephrol 16(8):2456–2461. doi:10.1681/ASN.2005020179

Hingorani AD (2001) Polymorphisms in endothelial nitric oxide synthase and atherogenesis: John French Lecture 2000. Atherosclerosis 154(3):521–527

Kavanaugh MP, Wang H, Zhang Z, Zhang W, Wu YN, Dechant E, North RA, Kabat D (1994) Control of cationic amino acid transport and retroviral receptor functions in a membrane protein family. J Biol Chem 269(22):15445–15450

Kielstein JT, Impraim B, Simmel S, Bode-Böger SM, Tsikas D, Frölich JC, Hoeper MM, Haller H, Fliser D (2004) Cardiovascular effects of systemic nitric oxide synthase inhibition with asymmetrical dimethylarginine in humans. Circulation 109(2):172–177. doi:10.1161/01.CIR.0000105764.22626.B1

Kitiyakara C, Chabrashvili T, Jose P, Welch WJ, Wilcox CS (2001) Effects of dietary salt intake on plasma arginine. Am J Physiol Regul Integr Comp Physiol 280(4):R1069–R1075

Koepsell H, Lips K, Volk C (2007) Polyspecific organic cation transporters: structure, function, physiological roles, and biopharmaceutical implications. Pharm Res 24(7):1227–1251. doi:10.1007/s11095-007-9254-z

König J, Zolk O, Singer K, Hoffmann C, Fromm MF (2011) Double-transfected MDCK cells expressing human OCT1/MATE1 or OCT2/MATE1: determinants of uptake and transcellular translocation of organic cations. Br J Pharmacol 163(3):546–555. doi:10.1111/j.1476-5381.2010.01052.x

Mann GE, Yudilevich DL, Sobrevia L (2003) Regulation of amino acid and glucose transporters in endothelial and smooth muscle cells. Physiol Rev 83(1):183–252. doi:10.1152/physrev.00022.2002

Mateus A, Matsson P, Artursson P (2013) Rapid measurement of intracellular unbound drug concentrations. Mol Pharm. doi:10.1021/mp4000822

Meyer zu Schwabedissen HE, Verstuyft C, Kroemer HK, Becquemont L, Kim RB (2010) Human multidrug and toxin extrusion 1 (MATE1/SLC47A1) transporter: functional characterization, interaction with OCT2 (SLC22A2), and single nucleotide polymorphisms. Am J Physiol Renal Physiol 298(4):F997–F1005. doi:10.1152/ajprenal.00431.2009

Müller F, König J, Glaeser H, Schmidt I, Zolk O, Fromm MF, Maas R (2011) Molecular mechanism of renal tubular secretion of the antimalarial drug chloroquine. Antimicrob Agents Chemother 55(7):3091–3098. doi:10.1128/AAC.01835-10

Nicholson B, Manner CK, Kleeman J, MacLeod CL (2001) Sustained nitric oxide production in macrophages requires the arginine transporter CAT2. J Biol Chem 276(19):15881–15885. doi:10.1074/jbc.M010030200

Nickovic V, Nikolic J, Djindjic N, Ilic M, Nickovic J, Mladenovic D, Krstic N (2012) Diagnostical significance of dimethylarginine in the development of hepatorenal syndrome in patients with alcoholic liver cirrhosis. Vojnosanit Pregl 69(8):686–691

Nijveldt RJ, Van Leeuwen PA, Van Guldener C, Stehouwer CD, Rauwerda JA, Teerlink T (2002) Net renal extraction of asymmetrical (ADMA) and symmetrical (SDMA) dimethylarginine in fasting humans. Nephrol Dial Transplant 17(11):1999–2002

Ohta KY, Imamura Y, Okudaira N, Atsumi R, Inoue K, Yuasa H (2009) Functional characterization of multidrug and toxin extrusion protein 1 as a facilitative transporter for fluoroquinolones. J Pharmacol Exp Ther 328(2):628–634. doi:10.1124/jpet.108.142257

Otsuka M, Matsumoto T, Morimoto R, Arioka S, Omote H, Moriyama Y (2005) A human transporter protein that mediates the final excretion step for toxic organic cations. Proc Natl Acad Sci USA 102(50):17923–17928. doi:10.1073/pnas.0506483102

Palm F, Friederich M, Carlsson PO, Hansell P, Teerlink T, Liss P (2008) Reduced nitric oxide in diabetic kidneys due to increased hepatic arginine metabolism: implications for renomedullary oxygen availability. Am J Physiol Renal Physiol 294(1):F30–F37. doi:10.1152/ajprenal.00166.2007

Perkins CP, Mar V, Shutter JR, del Castillo J, Danilenko DM, Medlock ES, Ponting IL, Graham M, Stark KL, Zuo Y, Cunningham JM, Bosselman RA (1997) Anemia and perinatal death result from loss of the murine ecotropic retrovirus receptor mCAT-1. Genes Dev 11(7):914–925

Pietig G, Mehrens T, Hirsch JR, Cetinkaya I, Piechota H, Schlatter E (2001) Properties and regulation of organic cation transport in freshly isolated human proximal tubules. J Biol Chem 276(36):33741–33746. doi:10.1074/jbc.M104617200

Rodionov RN, Murry DJ, Vaulman SF, Stevens JW, Lentz SR (2010) Human alanine-glyoxylate aminotransferase 2 lowers asymmetric dimethylarginine and protects from inhibition of nitric oxide production. J Biol Chem 285(8):5385–5391. doi:10.1074/jbc.M109.091280

Ronden RA, Houben AJ, Teerlink T, Bakker JA, Bierau J, Stehouwer CD, De Leeuw PW, Kroon AA (2012) Reduced renal plasma clearance does not explain increased plasma asymmetric dimethylarginine in hypertensive subjects with mild to moderate renal insufficiency. Am J Physiol Renal Physiol 303(1):F149–F156. doi:10.1152/ajprenal.00045.2012

Siroen MP, Warle MC, Teerlink T, Nijveldt RJ, Kuipers EJ, Metselaar HJ, Tilanus HW, Kuik DJ, van der Sijp JR, Meijer S, van der Hoven B, van Leeuwen PA (2004) The transplanted liver graft is capable of clearing asymmetric dimethylarginine. Liver Transpl 10(12):1524–1530. doi:10.1002/lt.20286

Siroen MP, van der Sijp JR, Teerlink T, van Schaik C, Nijveldt RJ, van Leeuwen PA (2005) The human liver clears both asymmetric and symmetric dimethylarginine. Hepatology 41(3):559–565. doi:10.1002/hep.20579

Strobel J, Mieth M, Endress B, Auge D, König J, Fromm MF, Maas R (2012) Interaction of the cardiovascular risk marker asymmetric dimethylarginine (ADMA) with the human cationic amino acid transporter 1 (CAT1). J Mol Cell Cardiol 53(3):392–400. doi:10.1016/j.yjmcc.2012.06.002

Tang J, Frankel A, Cook RJ, Kim S, Paik WK, Williams KR, Clarke S, Herschman HR (2000) PRMT1 is the predominant type I protein arginine methyltransferase in mammalian cells. J Biol Chem 275(11):7723–7730

Teerlink T, Luo Z, Palm F, Wilcox CS (2009) Cellular ADMA: regulation and action. Pharmacol Res 60(6):448–460. doi:10.1016/j.phrs.2009.08.002

Tojo A, Welch WJ, Bremer V, Kimoto M, Kimura K, Omata M, Ogawa T, Vallance P, Wilcox CS (1997) Colocalization of demethylating enzymes and NOS and functional effects of methylarginines in rat kidney. Kidney Int 52(6):1593–1601

Tsikas D, Böger RH, Sandmann J, Bode-Böger SM, Fröhlich JC (2000) Endogenous nitric oxide synthase inhibitors are responsible for the L-arginine paradox. FEBS Lett 478(1–2):1–3

Tsuda M, Terada T, Asaka J, Ueba M, Katsura T, Inui K (2007) Oppositely directed H+ gradient functions as a driving force of rat H+/organic cation antiporter MATE1. Am J Physiol Renal Physiol 292(2):F593–F598. doi:10.1152/ajprenal.00312.2006

Vallance P, Leiper J (2004) Cardiovascular biology of the asymmetric dimethylarginine:dimethylarginine dimethylaminohydrolase pathway. Arterioscler Thromb Vasc Biol 24(6):1023–1030. doi:10.1161/01.ATV.0000128897.54893.26

Vallance P, Leone A, Calver A, Collier J, Moncada S (1992) Accumulation of an endogenous inhibitor of nitric oxide synthesis in chronic renal failure. Lancet 339(8793):572–575. doi:10.1016/0140-6736(92)90865-Z

Visigalli R, Barilli A, Bussolati O, Sala R, Gazzola GC, Parolari A, Tremoli E, Simon A, Closs EI, Dall'Asta V (2007) Rapamycin stimulates arginine influx through CAT2 transporters in human endothelial cells. Biochim Biophys Acta 1768(6):1479–1487. doi:10.1016/j.bbamem.2007.02.016

White MF, Christensen HN (1982) The two-way flux of cationic amino acids across the plasma membrane of mammalian cells is largely explained by a single transport system. J Biol Chem 257(17):10069–10080

Winter TN, Elmquist WF, Fairbanks CA (2011) OCT2 and MATE1 provide bidirectional agmatine transport. Mol Pharm 8(1):133–142. doi:10.1021/mp100180a

Zoccali C, Bode-Böger S, Mallamaci F, Benedetto F, Tripepi G, Malatino L, Cataliotti A, Bellanuova I, Fermo I, Frölich J, Böger R (2001) Plasma concentration of asymmetrical dimethylarginine and mortality in patients with end-stage renal disease: a prospective study. Lancet 358(9299):2113–2117

Zolk O, Solbach TF, König J, Fromm MF (2009) Structural determinants of inhibitor interaction with the human organic cation transporter OCT2 (SLC22A2). Naunyn Schmiedebergs Arch Pharmacol 379(4):337–348. doi:10.1007/s00210-008-0369-5